

## Heralding quantum entanglement between two room-temperature atomic ensembles: supplement

**HANG LI,<sup>1,2</sup> JIAN-PENG DOU,<sup>1,2</sup> XIAO-LING PANG,<sup>1,2</sup> TIAN-HUAI YANG,<sup>1,2</sup> CHAO-NI ZHANG,<sup>1,2</sup> YUAN CHEN,<sup>1,3</sup> JIA-MING LI,<sup>4,8</sup> IAN A. WALMSLEY,<sup>5,6</sup>  AND XIAN-MIN JIN<sup>1,2,7,\*</sup> **

<sup>1</sup>Center for Integrated Quantum Information Technologies (IQIT), School of Physics and Astronomy and State Key Laboratory of Advanced Optical Communication Systems and Networks, Shanghai Jiao Tong University, Shanghai 200240, China

<sup>2</sup>CAS Center for Excellence and Synergetic Innovation Center in Quantum Information and Quantum Physics, University of Science and Technology of China, Hefei, Anhui 230026, China

<sup>3</sup>Institute for Quantum Science and Engineering and Department of Physics, Southern University of Science and Technology, Shenzhen 518055, China

<sup>4</sup>School of Physics and Astronomy, Shanghai Jiao Tong University, Shanghai 200240, China

<sup>5</sup>Clarendon Laboratory, University of Oxford, Parks Road, Oxford OX1 3PU, UK

<sup>6</sup>Blackett Laboratory, Imperial College London, London SW7 2AZ, UK

<sup>7</sup>TuringQ Co., Ltd., Shanghai 200240, China

<sup>8</sup>e-mail: [lijm@sjtu.edu.cn](mailto:lijm@sjtu.edu.cn)

\*Corresponding author: [xianmin.jin@sjtu.edu.cn](mailto:xianmin.jin@sjtu.edu.cn)

---

This supplement published with The Optical Society on 17 June 2021 by The Authors under the terms of the [Creative Commons Attribution 4.0 License](https://creativecommons.org/licenses/by/4.0/) in the format provided by the authors and unedited. Further distribution of this work must maintain attribution to the author(s) and the published article's title, journal citation, and DOI.

Supplement DOI: <https://doi.org/10.6084/m9.figshare.14663868>

Parent Article DOI: <https://doi.org/10.1364/OPTICA.424599>

# Heralding Quantum Entanglement between Two Room-Temperature Atomic Ensembles

This document provides supplementary information to "Heralding Quantum Entanglement between Two Room-Temperature Atomic Ensembles", giving the details about the experiments.

## 1. EXPERIMENTAL DETAILS

As the entire experimental setup shows in Figure 2 of the main text, the two  $^{133}\text{Cs}$  cells, separated by 30 cm, are placed into a magnetic shielding and heated to 61°C for getting a large optical depth. In order to alleviate the collisions between cesium atoms, we have injected 10 Torr Ne buffer gas into the vapor cell. Benefit from the developed precise frequency locking system, the frequency of the optical control light can be locked to a fixed detuning and conveniently tuned on demand, which helps to create and verify the quantum entanglement precisely. The pump light, being resonated to the  $|e\rangle \rightarrow |s\rangle$  transition, is directed from one port of Wollaston prism (WP), which propagates along the same path of the optical control light but with opposite direction and is employed to initialize the state of atoms. The creation of the pump and control light is generated in a programable fashion. To be specific, the optical control light pulse is 2ns generated by a high speed light modulator and the pump light pulse is 2us propagating along the diffraction path of an acousto-optical modulators (AOM). The Stokes and anti-Stokes photons generated via far off-resonance spontaneous Raman scattering process are orthogonally polarized with the optical pump and probe light [1]. We separate the control light and signal photons by their polarization via a high-extinction WP, which increases the signal-to-noise ratio for the Stokes and anti-Stokes photons. Besides the polarization filtering, we have built four sets of broadband Fabry-Pérot cavities to extract the signal photons from the noise, whose single cavity can reach the transmission rate of 92% and the extinction rate of 500 : 1. The Stokes and anti-Stokes photons are detected by the single-photon detectors, which are the silicon avalanche photodiodes from Excelitas Technologies with 50% detection efficiency.

The optical control pulse is directed into the Mach-Zehnder interferometer to generate the entanglement between the L and R ensembles. For combine photons from two ensembles at the PBS, the polarization of the control light in the left arm is transformed into being orthogonal to the right arm by the HWP after the GTP. The continuous auxiliary light field for phase locking is paralleled to the path of the control light, but has a small spatial shift to go thorough the hollow HWP for changing its polarization. This design is mainly due to the orthogonal polarizations between the control light passing through the GTP and the scattered signal photons passing the port of WP. The interference results of the auxiliary light field will be input to the processor, and then a feedback electric signal will be given to drive PZT to actively lock the phase of the interferometer. In order to analyze the correlated photon pairs with individual modules (i.e. the heralding part and verifying part, as shown in the Figure 2 of the main text), the Stokes and anti-Stokes photon are separated with their time sequences by applying a 100 ns controlling signal to the AOM, in which the anti-Stokes photons pass through the way along the original incident direction and the Stokes photons propagate along the diffraction path. The PS is used to adjust the Pancharatnam-Berry's phase to acquire the interference results of the heralded anti-Stokes photon.

## 2. THE PERFORMANCE OF DLCZ PROTOCOL OPERATED IN EACH QUANTUM NODE.

Before performing the heralding entanglement experiment, we need to characterize the performance of each atomic ensemble operated in the far off-resonance Duan-Lukin-Cirac-Zoller(DLCZ) protocol. The excitation probability is defined as  $\lambda = \frac{N_s}{N_{all}}$ , labelled as  $\lambda_L$  and  $\lambda_R$  for the L/R ensembles, where the  $N_s$  is the counts of Stokes photons and  $N_{all}$  is the total trials in the counting period. The retrieval efficiency is defined as  $q = \frac{N_{s,as}}{N_s}$ , labelled as  $q_L$  and  $q_R$  for the L/R ensembles, where the  $N_{s,as}$  is the coincidence counts between the Stokes photons and anti-Stokes photons. From the raw data, we can measure that  $\lambda_L = 4.2 \times 10^{-4}$  and  $\lambda_R = 4.7 \times 10^{-4}$ , and  $q_L = 3.1 \times 10^{-3}$  and  $q_R = 3.5 \times 10^{-3}$ . The above data are analyzed by the original experimental

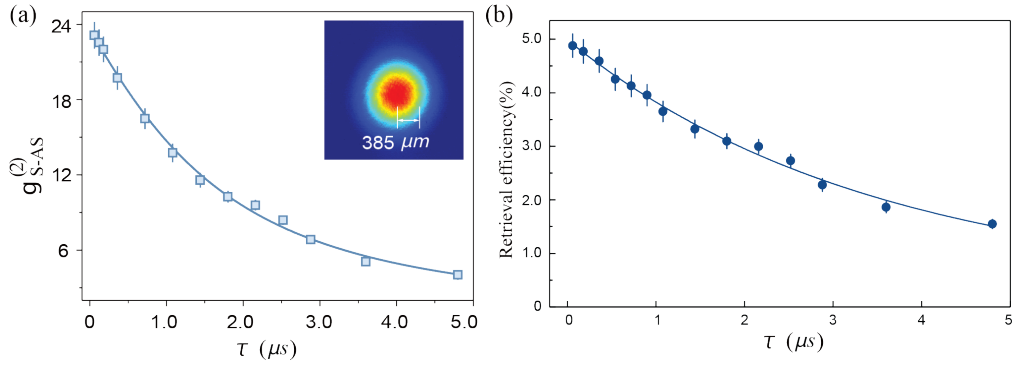


**Fig. S1. The lifetime of built-in quantum memory.** The fitting results of memory lifetime, and the optical control beam waist of  $385\mu\text{m}$  shown in the inset. **a.** The memory lifetime is measured as the decay of the cross-correlation functions, which is estimated as  $2.24\mu\text{s}$ . **b.** The memory lifetime is measured as the decay of the retrieval efficiency, which is estimated as  $3.50\mu\text{s}$ .

counting record, which includes the influences of the loss caused by coupling, filtering and detectors. During the standard DLCZ protocol, the retrieval anti-Stokes photon is heralded by the Stokes photon generated from the write process, then we need to measure the cross-correlation function between this correlated photons pair, labelled by  $g_{S,AS}^{(2)L}$  and  $g_{S,AS}^{(2)R}$  for the L/R ensembles. If the cross-correlation function value is higher than 2, it means that there will be non-classical correlation between them. The higher cross-correlation function value means the lower noise level in the retrieval process. The measured results are  $g_{S,AS}^{(2)L} = 27.98 \pm 1.75$  and  $g_{S,AS}^{(2)R} = 26.89 \pm 1.75$  with the storage time of  $100\text{ns}$ , which are far exceed the key boundary of 6 (above which quantum correlation are able to violate Bell's inequality).

The lifetime of our built-in quantum memory can be defined as the value of cross-correlation dropping to  $1/e$ . To alleviate the decoherence caused by atomic motion and avoid the atoms from getting away from the interaction region, we adopt a large beam waist of the optical control beam with  $385\mu\text{m}$ . Therefore, it needs more time for excited atoms to run out of interaction region, which may bring longer lifetime for the far off-resonance quantum memory, as is shown in Fig. S1. We can fit the experimental data by the function of  $g^{(2)}(\tau) = 1 + C/(1 + A\tau + B\tau^2)$  [2], where quadratic term comes from atomic motion, and linear term S-AS comes from background noise, and get the lifetime about  $2.24\mu\text{s}$ . In addition, the spatial mode of optical control field is also optimized as Gaussian beams, which is shown in the inset of Fig. S1. There is another usually adopted way to estimate the lifetime is to measure the decay of the retrieval efficiency with time, so we can also give the memory lifetime as  $3.50\mu\text{s}$  in this way.

### 3. THE PHASE LOCKING FOR HETERO-BEAM WITH ORTHOGONAL POLARIZATION

The phase stabilization is necessary for faithful and stable observation of the interference of the heralded entanglement of different anti-Stokes modes. Either the phase  $\varphi_S$  or  $\varphi_{AS}$  contains two similar components, i.e. the phase difference resulting from the optical pump or probe pulse at two ensembles, i.e. the phase difference accumulated from the propagation of Stokes or anti-Stokes photon. Due to the slowly drift of temperature or mechanical vibrations of optical devices at the ambient environment, the phases about the propagation of signal photons (the Stokes and anti-Stokes photons) will suffer from dramatic variations. In order to observe and verify the genuine entanglement between the two room-temperature ensembles from trial to trial, we should stabilize the interferometer loop in Figure 2 (see the main text) at a fixed phase.

The auxiliary light field for phase locking of the interferometer loop in Figure 2 of the main text has the same frequency as optical pump and probe pulse, but in the form of continuous wave. The purpose of the "hollow halfwave-plate" is to change the polarization of the auxiliary light field for phase locking after passing through it, but not influence the polarization of the optical control fields. For the purpose of stabilizing the phase of the whole Mach-Zehnder interferometer in Figure 2, the auxiliary light field for phase locking should experience the same path as the Stokes/anti-Stokes photons go through. Due to the orthogonal polarization between the optical

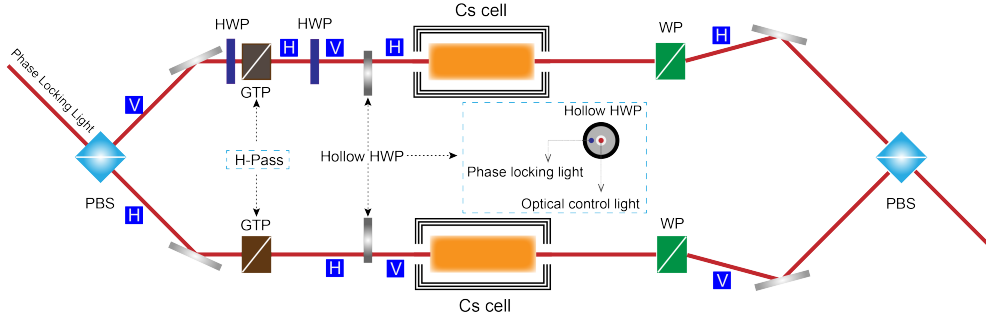


**Fig. S2. The scheme of phase locking.** For combine photons from two ensembles at the PBS, the polarization of the control light in the left arm is transformed into being orthogonal to the right arm by the HWP after the GTP. The continuous auxiliary light field for phase locking will go through the hollow HWP to change its polarization, while the paralleled control light will go through the hollow part of hollow HWP with its polarization unchanged. The variations of polarization have been marked in the blue square along the optical path. PBS: polarization beam splitter, WP: Wollaston prism, GTP: Glan-Taylor prism, HWP: half wave plate.

control light and scattering Stokes/anti-Stokes photons, it is impossible to make the auxiliary light field propagating through the same path in the original interferometer loop if there doesn't have the "hollow halfwave-plate", because the Glan-Taylor prism used for purifying the polarization of control light only allows the horizontally polarized light pass through, and redirects the light with vertical polarization into another direction in a extinction rate up to  $10^5$ . As the FIG S2 shows, the auxiliary light field passing through the Glan-Taylor prism is still in the horizontal polarization and it will go to the same port of Wollaston prism as the optical control field without the "hollow halfwave-plate", which is not the port of Stokes/anti-Stokes photons going through. Therefore, we have developed this type of halfwave-plate to change the polarization of the auxiliary light field but leave the optical control fields unchanged by passing through the hollow region of this "hollow halfwave-plate" and the two fields will be parallel with a small spatial shift as the subgraph depicted in Fig S2. According to the interference results of the auxiliary field, the feedback electric controlling signal will be sent to the Piezoelectric ceramics to compensate the optical path.

#### 4. QUANTUM INTERFERENCE FOR THE HERALDED ENTANGLEMENT OF ANTI-STOKES MODES

The "On/Off detection" means that the APD detector can not give the information of photon numbers in the trial of one-shot detection but give the result that has already registered the arriving of photons. If one would like to confirm this detection is a single photon, which can be analyzed in the standard HBT configuration. The detectors D1 and D2 will herald entanglement upon detection of a Stokes photon in either of the two orthogonal polarizations, which can project the data sets into two groups. The Figure 3 of main manuscript has shown the post-select data set heralded by D1 and the data set heralded by D2 has similar interference result.

For evaluating the coherence of the heralded superposition modes between the orthogonal polarization of anti-Stokes photon (can be written as  $\frac{1}{\sqrt{2}} (|H\rangle_L^{AS} \pm e^{i\varphi_{AS}} |V\rangle_R^{AS})$ ), we need to control the phase  $\varphi_{AS}$  to acquire the interference results by means of the projection measurements (made up of the half-wave plate and polarizing beamsplitter shown in Figure 2 of the main text). The  $\varphi_{AS}$  between the  $|H\rangle$  and  $|V\rangle$  basis can be manipulated by the Pancharatnam-Berry's phase [3–5], which is a wave plates combination in the configuration of QWP-HWP-QWP (labelled by the component phase shifter in the verifying module of Figure 2). Through this wave plate settings, we can implement an arbitrary rotation around the  $z$  axis in the Bloch sphere and this unitary rotation is given by:

$$R_z(\theta) = U_{qwp}(\frac{\pi}{4})U_{hwp}(-\frac{\pi}{4} - \frac{\theta}{4})U_{qwp}(\frac{\pi}{4}) = \begin{bmatrix} e^{-i\frac{\theta}{2}} & 0 \\ 0 & e^{i\frac{\theta}{2}} \end{bmatrix} \quad (S1)$$

where  $\theta$  is the angle to be rotated around the Bloch sphere,  $U$  represents the unitary operation by

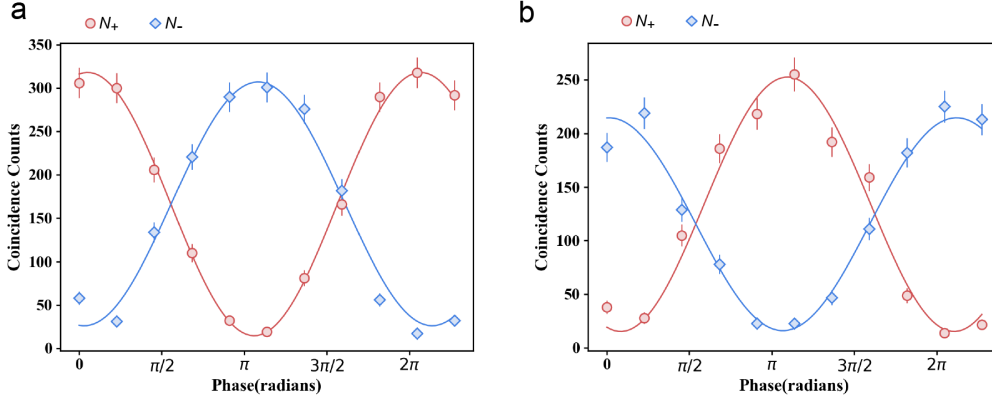


**Fig. S3. The full data set heralded by both  $D_{1/2}$  with the Storage time of 200ns.** **a.** Coincidence counts heralded by the Stokes detection of  $D_1$ , where  $N_+$  counts the number of  $D_3$  events conditioned on  $D_1$  events, and  $N_-$  counts coincidences between  $D_4$  and  $D_1$  in the same trial. The estimates of visibilities for  $N_{\pm}$  is  $V_+ = (91 \pm 1)\%$  for  $N_+$ , and  $V_- = (84 \pm 2)\%$  for  $N_-$ . **b.** Coincidence counts heralded by the Stokes detection of  $D_2$ , where  $N_+$  counts the number of  $D_3$  events conditioned on a  $D_2$  event, and  $N_-$  counts coincidences between  $D_4$  and  $D_2$  in the same trial. The estimates of visibilities for  $N_{\pm}$  is  $V_+ = (88 \pm 2)\%$  for  $N_+$ , and  $V_- = (86 \pm 2)\%$  for  $N_-$ .

the QWP or HWP. From the component of rotation matrix  $R_z(\theta)$ , the angle of both QWP should be set in  $45^\circ$  and the rotation angle  $\theta$  is adjusted by the middle HWP, while each  $\theta$  rotation of HWP corresponds to adding  $4\theta$  in the phase between the orthogonal anti-Stokes modes.

We have also measured the coincidence counts between the heralding Stokes photons and the read-out anti-Stokes photons with the storage time of 200ns. The full data set heralded by both  $D_{1/2}$  detectors are shown in Fig S3. The imbalanced coincidence counts between the heralded data of  $D_1$  and  $D_2$  is mainly resulted from the slightly different detecting efficiency about the Stokes photons in the paths of  $D_1$  and  $D_2$ , where the detecting efficiency is composed of the coupling efficiency, the filtering efficiency, and the efficiency of detectors, as the Figure 2 in the main text shows. In this case, we can estimate that the average visibilities are 88% for the data heralded by  $D_1$  and 87% for the data heralded by  $D_2$ . The measured  $p_{01} = 3.07 \times 10^{-3}$ ,  $p_{10} = 3.35 \times 10^{-3}$  and  $p_{11} = (5.5 \pm 1.1) \times 10^{-7}$ , so we can estimate the  $d = V \times (p_{01} + p_{10})/2 = 2.82 \times 10^{-3}$  for the data heralded by  $D_1$  and  $d = 2.79 \times 10^{-3}$  for  $D_2$ . As the main text in Figure 3 does, we can provide an evaluation of the concurrence as  $C_p^{D_1} = (4.2 \pm 0.3) \times 10^{-3}$ ,  $C_p^{D_2} = (4.1 \pm 0.3) \times 10^{-3}$ .

## REFERENCES

1. Nunn, J, Quantum Memory in Atomic Ensembles. Ph.D. thesis, University of Oxford, 481-487 (2008).
2. Zhao, B. *et al.* A millisecond quantum memory for scalable quantum networks. *Nature Phys.* **5**, 95-99 (2009).
3. K. C. Lee, *et al.* Entangling Macroscopic Diamonds at Room Temperature. *Science*. **334**, 1253 (2011).
4. M. V. Berry, Quantal Phase Factors Accompanying Adiabatic Changes, Proceedings of the Royal Society of London. A. Mathematical and Physical Sciences, **392**, pp. 45-57 (1984).
5. N. K. Langford, Encoding, manipulating and measuring quantum information in optics, Ph.D. thesis, School of Physical Sciences, University of Queensland (2007).
6. Clauser, J. F., Horne, M. A., Shimony, A. & Holt, R. A. Proposed experiment to test local hidden-variable theories. *Phys. Rev. Lett.* **23**, 880 (1969)
7. D. F. V. James, P. G. Kwiat, W. J. Munro, A. G. White, *Phys. Rev. A* **64**, 052312 (2001).
8. W. Wootters, *Phys. Rev. Lett.* **80**, 2245 (1998).
9. J. Laurat, *et al.* Heralded Entanglement between Atomic Ensembles: Preparation, Decoherence, and Scaling. *Phys. Rev. Lett.* **99**, 180504 (2007).